Main Group Metal Compounds   AOC

Synthesis, spectroscopic characterization and biocidal activity of some diorganotin(IV) complexes of salicylaldehydethiosemicarbazones and related ligands. Molecular and supramolecular structures of [R₂Sn(OArCH=N–N=CSNH₂)], where R = Me, Ph and Ar = – C₆H₄, –C₆H₃(5-Br) and C₆H₃(5-Cl), and of [Me₂Sn{OC₆H₃(5-Br)CH=N–N=CSNH₂}]·OH₂†

Moumita Sen Sarma[1], Shibnath Mazumder[2], Debabrata Ghosh[2], Abhijit Roy[1]*, Andrew Duthie[3] and Edward R. T. Tiekink[4]*

[1]Department of Chemistry, North Bengal University, Darjeeling, West Bengal 734430, India
[2]Immunobiology Laboratory, School of Life Sciences, Visva-Bharati, Santiniketan 731235, India
[3]School of Life and Environmental Sciences, Deakin University, Geelong 3217, Australia
[4]Department of Chemistry, The University of Texas at San Antonio, One UTSA Circle, San Antonio, TX 78249-0698, USA

Nine diorganotin(IV) compounds of Schiff bases derived from salicylaldehyde/substituted salicylaldehyde and thiosemicarbazide were synthesized. The compounds, with general formulae [R₂Sn(OArCH=N–N=CSNH₂)], where R = Me, *n*-Bu, Ph and Ar = – C₆H₄, –C₆H₃(5-Cl), –C₆H₃(5-Br), were characterized by UV and IR spectroscopy, NMR (¹H, ¹³C and ¹¹⁹Sn) spectroscopy and elemental analysis. X-ray crystallographic studies of five of these complexes indicate penta-coordination of tin within a distorted C₂NOS trigonal bipyramidal geometry in each case. The crystal packing in four of the structures features {· · · N–C–N–H}₂ synthons, but in [Ph₂Sn(OArCH=N–N=CSNH₂)] the {· · · S–C–N–H}₂ synthon is predominant. The biological activity of these compounds against four fungal pathogens (*Curvularia eragrostidis*, *Alternaria porri*, *Dreschlerea oryzae* and *Macrophomina phaseolina*) of four different crops (*Camellia sineusis*, *Guizotia abyssinica*, *Oryzae sativa* and *Solanum melongena*) and some bacteria (*Aeromonas hydrophila*, *Salmonella typhi*, *Salmonella typhimurium*, *Salmonella flexnri*, *Escheria coli*, *Salmonella aureus*, *Bacillus subtilis* and *Lactobacillus rhamnosus*) were investigated. Their cytotoxicity was also investigated against several human cancer cell lines. Copyright © 2007 John Wiley & Sons, Ltd.

KEYWORDS: tin(IV); organotin; crystal structure; biocidal activity; cytotoxicity; thiosemicarbazones

INTRODUCTION

Organotin compounds of O, N and S containing ligands are well known for their biological activity.[1–3] Amongst these

*Correspondence to: A. Roy, Department of Chemistry, North Bengal University, West Bengal, 734430, India; Edward R. T. Tiekink, Department of Chemistry, The University of Texas at San Antonio, One UTSA Circle, San Antonio, Texas 78249-0698, USA.
E-mail: abhijitchem1947@yahoo.co.in; Edward.Tiekink@tusa.edu
†Dedicated to the memory of Des Cunningham.

ligands, the chemistry of Schiff bases is of significant interest due to their structural diversity[4–6] and multidenticity.[7–9] Accordingly, much work has been done with these types of ligands[10–15] and the subject has also been reviewed.[16] The Schiff bases obtained by the condensation of salicylaldehyde and substituted salicylaldehydes with thiosemicarbazide form a class of versatile ONS donor ligands. Many studies of these latter molecules as ligands have so far dealt with transition metal complexes of thiosemicarbazone derivatives of salicylaldehyde and substituted salicylaldehydes,[17–20]

WILEY InterScience®
DISCOVER SOMETHING GREAT

whereby they stabilize unusual oxidation states and exhibit different coordination numbers in their complexes. For example, recently an unusual coordination mode of salicylaldehyde thiosemicarbazone was observed in a group of [M(PPh$_3$)$_2$(saltsc)$_2$] complexes, where M = Ru, Os and saltsc = anion of salicylaldehyde thiosemicarbazone.[21,22] Thiosemicarbazones and related ligands are reported to bind a metal ion as a monoanionic bidentate ligand coordinating through N and S atoms forming a five-membered chelate ring.[23,24] Our continued interest in these ligands led us to investigate the ligating behaviour of the versatile thiosemicarbazones towards the organotin moieties.[25] Herein, the synthesis, characterization and structures of diorganotin(IV) compounds of salicylaldehyde and substituted salicylaldehyde thiosemicarbazones are reported. Organotin compounds have been used as agricultural biocides.[26] Besides the high fungicidal and bactericidal properties,[1] various organotin compounds have been reported to possess anti-tumour activity with some derivatives being even more active than cisplatin.[27,28] The present work was also motivated by the desire to study the biocidal activity and cytotoxicty of these newly synthesized organotins. It is to be noted that during the progress of this work we became aware of reports of closely related studies[29–31] where some organotin(IV) complexes of semi- and thiosemicarbazones, along with the compounds **1**–**3** (Scheme 1), were described as well as their molecular structures.[30,31] These have been included herein to allow comparison of their biocidal properties with the corresponding Cl/Br-substituted ligands and because the compounds were synthesized via a different route, requiring shorter reaction times and giving higher yields. Further, full details of their supramolecular structures are reported as well as a correlation of geometric parameters with those of the halide congeners.
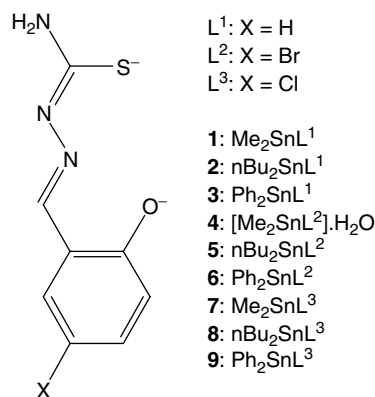
EXPERIMENTAL

General comments

Salicylaldehyde (Fluka AG, Switzerland), 5-chlorosalicylaldehyde (Lancaster, USA), 5-bromosalicylaldehyde (Lancaster, USA), thiosemicarbazide (Loba Chemie, India), *n*-dibutyltinoxide (Alfa, USA), Me$_2$SnCl$_2$ (Fluka, Germany), Ph$_2$SnCl$_2$ (Aldrich, USA) and *n*-Bu$_2$SnCl$_2$ (Merck, Germany) were used as received from commercial sources. Me$_2$SnO and Ph$_2$SnO were prepared by the alkaline hydrolysis of Me$_2$SnCl$_2$ and Ph$_2$SnCl$_2$ respectively in water–ether mixtures. The solvents used in the reactions were of AR grade and were obtained from commercial sources (Merck, Germany). The solvents were dried using standard literature procedures. Proper precautions were undertaken while working with benzene as a solvent.

Measurements

IR spectra in the range 4000–250 cm^{-1} were recorded on Pye-Unicam SP 300S spectrophotometer as Nujol mulls using

L^1: X = H
L^2: X = Br
L^3: X = Cl

1: Me$_2$SnL^1
2: nBu$_2$SnL^1
3: Ph$_2$SnL^1
4: [Me$_2$SnL^2].H$_2$O
5: nBu$_2$SnL^2
6: Ph$_2$SnL^2
7: Me$_2$SnL^3
8: nBu$_2$SnL^3
9: Ph$_2$SnL^3

Scheme 1.

CsI optics. ^{1}H and ^{13}C NMR spectra were obtained in CDCl$_3$ and C$_6$D$_6$ using TMS as an internal standard on a Bruker DPX 300 spectrometer. The solution ^{119}Sn NMR spectra were measured in CDCl$_3$ solution at 149.05 MHz using a Jeol Eclipse Plus 400 spectrometer and were referenced against SnMe$_4$. Tin was estimated gravimetrically as SnO$_2$ using standard procedures. Microanalyses were performed at RSIC, NEHU, Shillong, India. The electronic spectra were recorded on a Shimadzu UV 240 spectrophotometer with methanol as the solvent. Fluorescence studies were carried out on Elico SL174 spectrofluorometer.

Syntheses

Preparation of Schiff base of salicylaldehyde/substituted salicylaldehyde from thiosemicarbazide

The thiosemicarbazones were prepared by reacting equimolar amounts of thiosemicarbazides and respective salicylaldehyde/substituted salicylaldehydes in a 1 : 1 ethanol–water mixture.[21] The products were recrystallized from ethanol. The formulae of the ligands and the abbreviations of the complexes are presented in Scheme 1.

Synthesis of dimethyltin(IV) salicylaldehydethiosemicarbazonate (1)

In a typical reaction run, to a solution of salicylaldehyde thiosemicarbazone (0.650 g, 3.33 mmol) in methanol was added dropwise 0.1 M methanolic NaOH (74 ml, 0.266 g, 6.65 mmol) under stirring. The reaction system was stirred for 2 h and then a methanolic solution of Me$_2$SnCl$_2$ (0.732 g, 3.33 mmol) was added. The fluorescent yellow reaction mixture was refluxed for 8 h under inert conditions. The volatiles were removed and the dry mass extracted with hot petroleum ether (60–80 °C, 50 ml). Slow cooling yielded yellow crystals of the desired product.

Diorganotin(IV) compounds **2** and **3** were prepared analogously using the appropriate diorganotin dichlorides and the sodium salt of the ligand. These diorganotin analogues have the same analytical composition as the products isolated previously by a different synthetic route.[29–31]

Synthesis of dimethyltin(IV) 5-bromosalicylaldehydethiosemicarbazonate (4)

A mixture of Me_2SnO (0.359 g, 2.18 mmol) and 5-bromosalicylaldehyde thiosemicarbazone (0.597 g, 2.18 mmol) in benzene (100 ml) was refluxed under inert conditions for 10 h, the water produced being removed azeotropically. The volatiles were removed from the fluorescent yellow reaction mixture and the dry mass extracted with hot petroleum ether (60–80 °C, 50 ml). Yellow crystals of the desired product were obtained by cooling the solution.

The remaining compounds (**5–9**) were prepared analogously using the appropriate diorganotin oxide and ligand.

Biological studies

Bacterial strains and determination of antibacterial properties

The organotin compounds studied were dissolved in 0.3% DMSO–water. Solutions were prepared fresh and the pH adjusted to 7.4. The bacterial strains used in the study were *Aeromonas hydrophila* strain 646 (MTCC, India, Gram-negative pathogenic), *Salmonella typhi* strain 737 (NICED, India, Gram-negative pathogenic), *Salmonella typhimurium* strain 3099 (NICED, Gram-negative pathogenic), *Salmonella flexnri* strain NK 2226 (NICED, Gram-negative pathogenic), *Escheria coli* strain 25 922 (NICED, Gram-negative pathogenic), *Salmonella aureus* (gift from M. K. Saha, Gram-negative pathogenic), *Bacillus subtilis* strain 6633 (ATCC, Gram-positive non-pathogenic) and *Lactobacillus rhamnosus* strain 1408 (ATCC, Gram-positive non-pathogenic). Bacteria were maintained in nutrient agar slant at 4 °C and for experimental use they were grown in a specific medium to log phase at optimal temperature.

The anti-bacterial properties of the organotins were evaluated by the disc-diffusion method.[32] Bacteria were grown to mid-log phase and spread on nutrient agar plates. Sterile filter discs containing different concentrations of the organotins in 20–40 µl were applied on the bacterial plates and incubated at optimal temperature for 24 h. The inhibition zones appearing around each disc were measured and the sensitivity determined from the zone diameters appearing on the plates based on NCCLS charts. When the bacteria gave a zone with diameter less than 13 mm in the presence of an organotin, it was interpreted as resistant (R), when the zone had a diameter of 15–16 mm, the bacteria were considered to have intermediate sensitivity (I) and a clear zone with diameter of 17 mm or more indicated a high degree of sensitivity towards the compound (S).

Fungicidal activity

The fungal strains used were gifts from The Department of Botany, University of North Bengal. The strains were *Curvularia eragrostidis*, *Alternaria porri*, *Dreschlerea oryzae* and *Macrophomina phaseolina*, and these were grown on potato–dextrose agar (PDA, HiMedia, India) medium at 28 ± 1 °C.

The fungicidal activities were determined following spore germination bioassay as described by Rouxel *et al.*[33] Purified eluents (10 µl) were placed on two spots 3 cm apart on a clean, grease-free slide and the solvent was allowed to evaporate. One drop of spore suspension (20 µl), prepared from 15-day-old cultures of the fungi, was added to the treated spots. The slides were incubated at 27 ± 1 °C for 24 h under humid conditions in Petri plates. Finally, after proper incubation period, one drop of a Cotton Blue–Lactophenol mixture was added to each spot to fix the germinated spores. The number of spores germinated compared with the germinated spores of control (where no chemicals were used) was calculated using an average of 300 spores per treatment. The minimum inhibitory concentration required for complete inhibition was recorded in units of micrograms per millilitre.

Phytotoxic effects

Oryzae sativa (IR-8, ICAR, India), *Lens culinaris*, and *Cicer aurantinum* were collected from the University Agricultural Research Institute, Visva-Bharati, and the phytotoxic effects of different organotins determined.[25] Briefly, seeds of different species were incubated with different concentration of organotins for different time periods. Following incubation, the seeds were washed with distilled water and incubated in aerated moist chambers for 96 h at 28 °C. The percentage of seed germination was calculated and compared with the results obtained with seeds dipped in DMSO–water as well as with those incubated in water only.

In vitro screening of cytotoxicity against human cancer cell lines

The cytotoxicities of the organotins reported herein were evaluated against the different human cancer cell lines mentioned below. The human cancer cell lines were maintained in DMEM (Gibco) containing 10% FBS supplemented with 1% penicillin-streptomycin solution. Tissue culture plates (96-well) were seeded with cancer cell suspensions at a final concentration of 1×10^5 cell per well and incubated at 37 °C for 24 h to allow the cells to adhere to the culture wells. The organotin compounds were added to the cells at final concentrations of 10, 20 and 40 µg ml^{-1}, respectively, and incubated further for 48 h. Following incubation, the cells were fixed by adding 50 µl of 50% TCA for 60 min at 4 °C. The fixed cells were washed, air dried and 50 µl of 0.4% sulforhodamine B (SRB, Sigma) dye added to each well and incubated for 20 min. Following incubation, the cells were washed with 1% acetic acid solution and air-dried. A 10 mM Tris-base (100 µl unbuffered) solution was added to each well and colour development recorded at 540 nm and subtracted from the background measurement at 690 nm.[34] Adriamycin (Sigma) was used as positive control in the assay.

Crystal structure determinations

Intensity data were measured for selected crystals of at 223 K on a Bruker AXS Smart CCD with graphite monochromatized Mo$K\alpha$ radiation (0.71069 Å) so that $\theta_{max} = 30.0/30.1°$. Each

structure was solved by heavy-atom methods[35] and refined[36] on F^2 with non-hydrogen atoms modelled with anisotropic displacement parameters, with hydrogen atoms in the riding model approximation and using a weighting scheme of the form $w = 1/[\sigma^2(F_o^2) + (aP)^2 + bP]$ where $P = (F_o^2 + 2F_c^2)/3$. Crystal data are given in Table 1. The numbering schemes are shown in Figs 1–5 and were drawn with ORTEP.[37] Diagrams of the supramolecular structures were generated with the aid of the DIAMOND[38] programme.

RESULTS AND DISCUSSION

Diorganotin derivatives **1**–**9** (Scheme 1) were obtained in moderate yields by equimolar reaction of either diorganotin(IV) oxides with the appropriate ligand or diorganotin(IV) chlorides with the sodium salt of the respective ligand; compound (**4**) was isolated as a monohydrate. The compounds are relatively stable in moist air and can be recrystallized from suitable organic solvents. Physical data are summarized in Table 2. The complexes are soluble in chloroform, methanol, acetone, n-hexane and benzene.
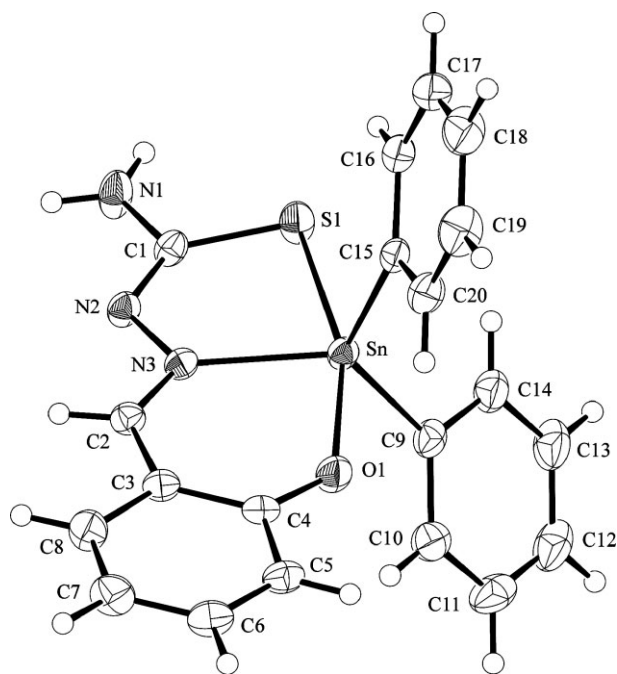
Crystal structures

Compounds **1**, **3**, **4**, **6** and **9** provided crystals suitable for X-ray crystal structure determination. The molecular structures
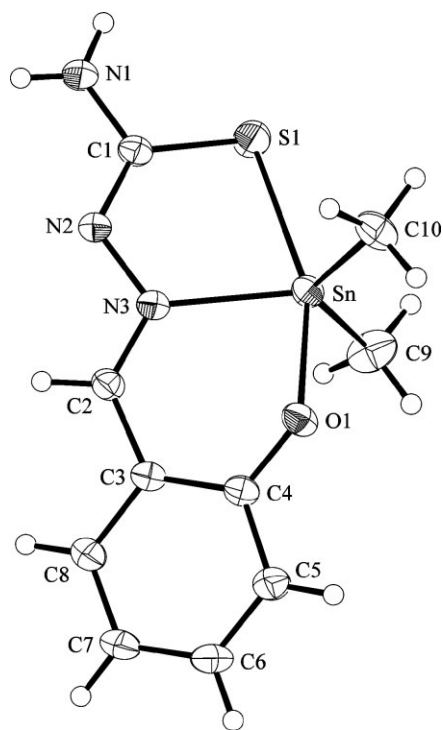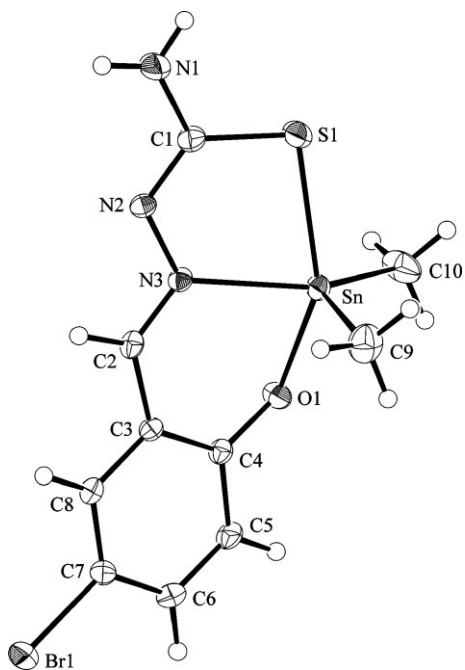

Figure 1. Molecular structure and crystallographic numbering scheme for [Me$_2$SnL^1] (**1**).

Table 1. Crystallographic data and refinement details for [Me$_2$SnL^1] (**1**), [Ph$_2$SnL^1] (**3**), [Me$_2$SnL^2]·H$_2$O (**4**), [Ph$_2$SnL^2] (**6**) and [Ph$_2$SnL^3] (**9**)

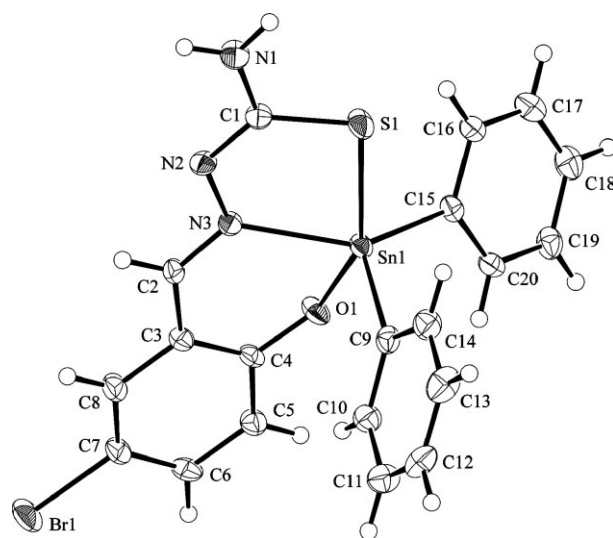|	**1**	**3**	**4**	**6**	**9**
Formula	C$_{10}$H$_{13}$N$_3$OSSn	C$_{20}$H$_{17}$N$_3$OSSn	C$_{10}$H$_{14}$BrN$_3$O$_2$SSn	C$_{20}$H$_{16}$BrN$_3$OSSn	C$_{20}$H$_{16}$ClN$_3$OSSn
Formula weight	341.98	466.12	438.90	545.02	500.56
Crystal system	Monoclinic	Monoclinic	Monoclinic	Triclinic	Triclinic
Space group	$P2_1/n$	$P2_1/c$	$C2/c$	P-1	P-1
a (Å)	9.4175(6)	15.5284(8)	15.5788(8)	12.7793(5)	8.8596(6)
b (Å)	13.4230(9)	10.0604(5)	13.6076(7)	12.8645(5)	9.9809(7)
c (Å)	10.5187(7)	13.3743(7)	13.9124(7)	13.5952(5)	12.7142(8)
α (deg)	90	90	90	93.877(2)	111.759(1)
β (deg)	100.266(1)	113.673(2)	93.936(2)	93.640(2)	109.741(1)
γ (deg)	90	90	90	118.031(2)	91.927(1)
V (Å^3)	1308.39(15)	1913.54(17)	2942.3(3)	1956.79(13)	966.44(11)
Z	4	4	8	4	2
D_c (g cm^{-3})	1.736	1.618	1.982	1.850	1.720
μ (MoKα, mm^{-1})	2.096	1.458	4.592	3.470	1.583
Measured data	10 789	15 651	12 167	16 439	8204
Unique data	3792	5538	4300	11 161	5504
Observed data					
[$I \geq 2.0\sigma(I)$]	3291	4188	3384	8228	4898
R, obs. data; all data	0.030; 0.036	0.035; 0.052	0.038; 0.054	0.053; 0.075	0.045; 0.051
a; b in weighting scheme	0.038; 0.431	0.040; 0	0.035; 0	0.077; 0.429	0.055; 0.497
R_w, obs. data; all data	0.075; 0.079	0.080; 0.087	0.080; 0.085	0.131; 0.142	0.103; 0.107
Largest residual (e Å^{-3})	0.85	0.86	1.13	4.78	1.45
CCDC deposition no.	638 421	638 422	638 423	638 424	638 425

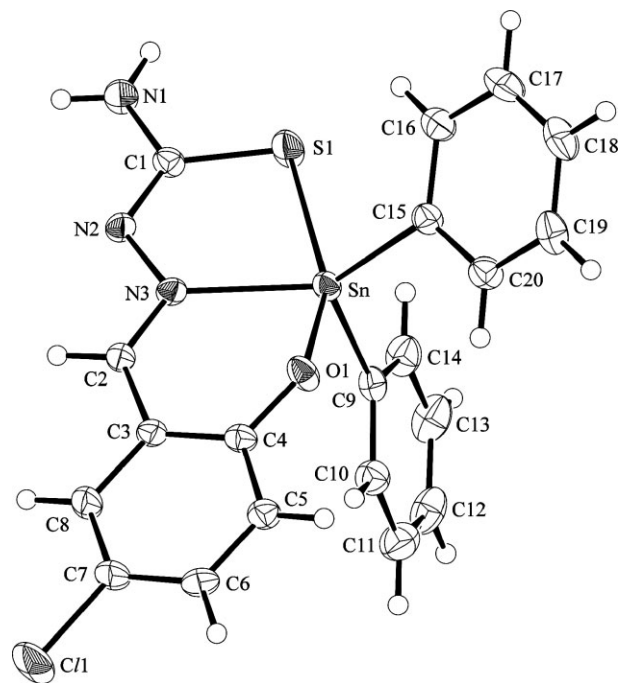**Figure 2.** Molecular structure and crystallographic numbering scheme for [Ph$_2$SnL^1] (**3**).

Figure 3. Molecular structure and crystallographic numbering scheme for [Me$_2$SnL^2].OH$_2$ (**4**). Water molecule of crystallization is omitted.

Figure 4. Molecular structure and crystallographic numbering scheme for one of the two independent molecules comprising the asymmetric unit of [Ph$_2$SnL^2] (**6**); the atomic labelling of the second independent molecule follows that as shown but with an added 'a' as a suffix.

Figure 5. Molecular structure and crystallographic numbering scheme for [Ph$_2$SnL^3] (**9**).

are shown in Figs 1–5 and selected geometric parameters are collected in Table 3. The structure of **1** features a five-coordinate tin atom coordinated by the S1, O1 and N3

atoms of the tridentate ligand as well as two methyl groups. The overall coordination geometry is based on a trigonal bipyramid with the S1 and O1 defining the axial positions. Distortions from the ideal geometry may be traced to the restraints imposed by the chelate rings. An examination of the

Table 2. Physical and analytical data for **1**–**9**[a]

	Yield (%)	M.p. (°C)	Elemental composition: found (calcd) (%)			
			C	H	N	Sn
1	85	152	34.59 (35.12)	3.78 (3.80)	12.27 (12.29)	34.60 (34.73)
2	80	93–94	45.01 (45.10)	5.85 (5.87)	9.79 (9.87)	27.69 (27.88)
3	70	131	51.45 (51.53)	3.61 (3.65)	9.00 (9.02)	25.40 (25.49)
4	75	111–113	27.29 (27.36)	3.12 (3.19)	9.55 (9.57)	26.99 (27.06)
5[b]	69	—	37.98 (38.04)	4.73 (4.75)	8.30 (8.32)	23.49 (23.52)
6	67	161–163	44.01 (44.06)	2.91 (2.93)	7.68 (7.71)	21.65 (21.79)
7	45	105–106	31.88 (31.90)	3.18 (3.19)	11.15 (11.16)	31.48 (31.55)
8[b]	65	—	41.05 (41.72)	5.18 (5.21)	9.10 (9.13)	25.69 (25.79)
9	48	169–171	47.90 (47.98)	3.18 (3.20)	8.38 (8.39)	23.61 (23.73)

[a] Reaction time was 8–10 h. All compounds are yellow. Compound **1** was crystallized from benzene while all others were obtained from petroleum ether (60–80 °C).
[b] Sticky liquid.

Table 3. Selected bond distances and angles for [Me_2SnL^1] (**1**), [Ph_2SnL^1] (**3**), [Me_2SnL^2].H_2O (**4**), [Ph_2SnL^2] (**6**) and [Ph_2SnL^3] (**9**)

|	1	3	4	6, 6a	9
Sn–S1	2.540(1)	2.546(1)	2.510(1)	2.494(1), 2.510(1)	2.500(1)
Sn–O1	2.105(2)	2.067(2)	2.103(2)	2.061(3), 2.071(3)	2.065(2)
Sn–N3	2.196(2)	2.191(2)	2.250(3)	2.265(3), 2.250(3)	2.250(3)
C1–S1	1.729(2)	1.738(3)	1.731(4)	1.740(4), 1.740(5)	1.732(4)
C1–N1	1.334(3)	1.349(3)	1.339(4)	1.350(5), 1.335(6)	1.340(4)
C1–N2	1.315(3)	1.298(3)	1.311(4)	1.313(5), 1.320(5)	1.312(4)
N2–N3	1.388(3)	1.387(3)	1.382(3)	1.388(5), 1.381(5)	1.394(3)
S1–Sn–O1	158.44(5)	161.31(6)	147.91(7)	150.1(1), 155.3(1)	152.28(8)
S1–Sn–N3	77.01(5)	77.94(5)	76.92(7)	77.11(9), 77.22(9)	77.40(7)
O1–Sn–N3	81.74(7)	84.22(7)	80.98(9)	80.8(1), 81.4(1)	80.92(9)
C9–Sn–C10	127.3(1)	—	118.5(2)	—	—
C9–Sn–C15	—	127.24(9)	—	118.0(2), 120.8(2)	118.7(1)

geometric parameters indicates that the structure conforms to the generic structure shown in Scheme 1, with no evidence of tautomerism. The molecular geometries of the remaining structures are in essential agreement with that just described and are in agreement with previous literature reports of the molecular structures of **1**–**3**, see the Introduction,[30,31] but have been determined to a higher level of precision owing to the benefit of modern equipment. Two independent molecules comprise the crystallographic asymmetric unit of **6** that differ from each other only in terms of minor conformational changes and the way they interact in the crystal structure (see below). The availability of a series of structures allows for the discernment of a number of trends in geometric parameters. From Table 3, it is evident that the inclusion of a halide substituent, i.e. chloride or bromide, at the C7 position results in significant stronger Sn–S bonds with concomitant weakening of the Sn–N3 bonds and greater deviation of the axial angle from 180 °C. A systematic variation in the Sn–O1 bonds is also apparent in that this bond is shorter in

the dimethyltin derivatives compared with the diphenyltin species. The presence of hydrogen bond donors and acceptors in each of the structures leads to a variety of supramolecular arrays and these are discussed in turn below.

In the crystal structure of [Me_2SnL^1] (**1**), N–H···O hydrogen bonding interactions lead to a chain along the *b*-axis and these are connected to neighbouring chains by N–H···N hydrogen bonds via eight-membered {···N–C–N–H}$_2$ synthons to form a two-dimensional array that has a zig-zag topology as highlighted in Fig. 6. The geometric parameters defining these interactions and those found in the remaining structures are listed in Table 4. The presence of tin-bound phenyl rings in [Ph_2SnL^1] (**3**) has a profound influence upon the supramolecular aggregation pattern as the oxygen atom now forms an intramolecular C–H···O contact that precludes its further association in the crystal structure. The global crystal packing may be described as comprising double layers of molecules that are connected via {···S–C–N–H}$_2$ synthons as shown in

Fig. 7. The remaining N–H atom participates in N–H$\cdots\pi$ contacts with tin-bound phenyl groups: an example is marked with an asterisk in Fig. 7. Finally, the imine-N2 atom participates in a C–H$\cdots$N interaction and thereby contributes to the stability of the aforementioned double layer. The structure of [Me$_2$SnL^2]$\cdot$H$_2$O (**4**) was isolated as a monohydrate and the water molecule plays a pivotal role in the crystal packing. Centrosymmetric molecules associate via the eight-membered $\{\cdots$N–C–N–H$\}_2$ synthon seen in compound **1**. These dimers are then linked into chains via an N1–H1b$\cdots$O2–H1w$\cdots$O1 sequence of hydrogen bonds and these chains are finally linked via weaker O–H$\cdots$O hydrogen bonds involving the water molecules exclusively; these are not shown in Fig. 8. As seen from the view in Fig. 8, this arrangement results in the formation of narrow channels aligned along the *c*-axis. Eight-membered $\{\cdots$N–C–N–H$\}_2$ synthons are the dominant intermolecular interactions found in the crystal structure of [Ph$_2$SnL^2] (**6**) and these occur between the two independent molecules comprising the asymmetric unit; these interactions are emphasized in Fig. 9.

Each of the remaining amine-H atoms is involved in an N–H$\cdots\pi$ interaction but rather than interacting with a ring system, each is orientated towards the C19–C20 bond of the other molecule comprising the dimer. Again, the oxygen atoms are shielded from forming intermolecular interactions owing to the presence of intramolecular C–H$\cdots$O contacts. The remaining interactions of note are of the type C–H$\cdots$Br, with the closest of these involving each independent bromide atom as listed in Table 4; those involving the Br2 atom are shown in Fig. 9. Finally, C–H$\cdots\pi$ contacts involving phenyl rings are noted. Although not isomorphous, the crystal packing found in [Ph$_2$SnL^3] (**9**) is similar to that just described for **6**. Hence, the $\{\cdots$N–C–N–H$\}_2$ synthon is present and these are connected to neighbouring molecules via N1–H1b$\cdots\pi$ (C19–C20) interactions. In this way, chains are formed which are linked via C–H$\cdots$Cl contacts. Two rows of chloride atoms align along the *a*-axis and interdigitate with each other, forming two C–H$\cdots$Cl contacts with molecules of the opposite row and resulting in the formation of a double zig-zag ribbon, Fig. 10.
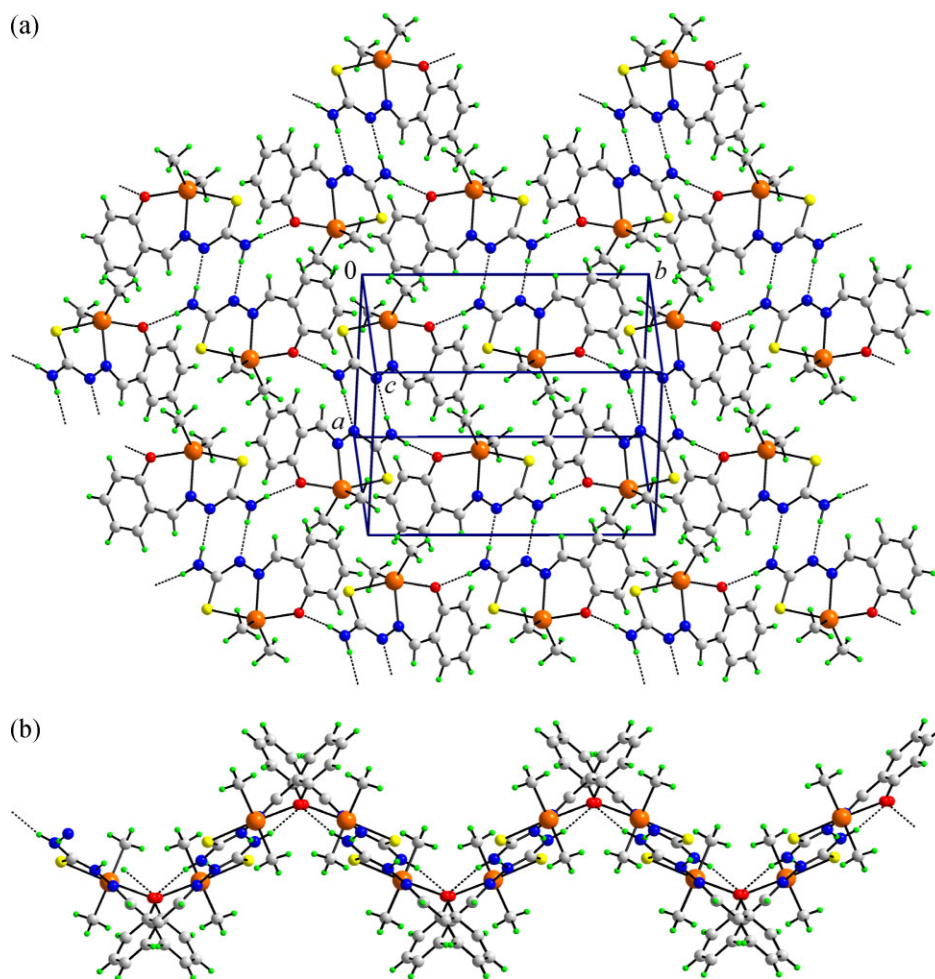
Figure 6. Crystal packing in [Me$_2$SnL^1] (**1**): (a) unit cell contents showing hydrogen bonding as dashed lines and (b) the zig-zag topology for the two-dimensional array. This figure is available in colour online at www.interscience.wiley.com/AOC.
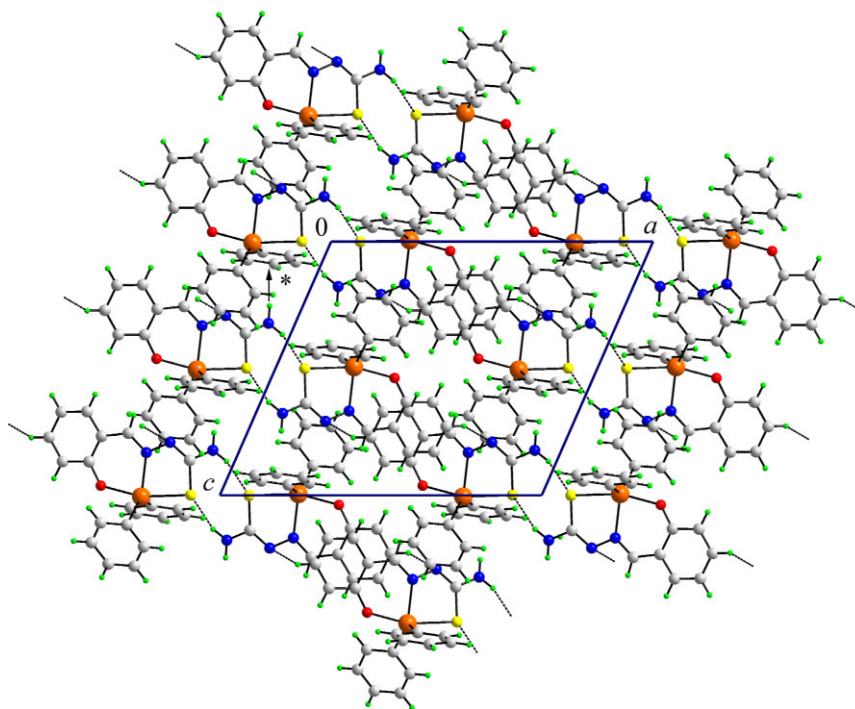
Figure 7. View of the unit cell contents of [Ph$_2$SnL^1] (**2**) along the *b*-axis. This figure is available in colour online at www.interscience.wiley.com/AOC.

Table 4. Summary of the major intermolecular interactions (A–H$\cdots$B; Å, °) operating in the crystal structures of [Me$_2$SnL^1] (**1**), [Ph$_2$SnL^1] (**3**), [Me$_2$SnL^2].H$_2$O (**4**), [Ph$_2$SnL^2] (**6**) and [Ph$_2$SnL^3] (**9**)

|	A	H	B	H$\cdots$B	A$\cdots$B	A–H$\cdots$B	Symmetry operation
1	N1	H1b	O1	2.03	2.866(3)	162	$1/2 - x, -1/2 + y, 1/2 - z$
	N1	H1a	N2	2.11	2.982(3)	176	$1 - x, -y, 1 - z$
3	N1	H1b	S1	2.77	3.507(3)	143	$-x, -y, -z$
	N1	H1a	Cg(C15–C20)^a	2.59	3.445(3)	167	$x, 1/2 - y, 1/2 + z$
	C6	H6	N2	2.55	3.345(4)	143	$1 - x, 1/2 + y, 1/2 - z$
4	N1	H1a	N2	2.23	3.102(4)	177	$1 - x, -y, -z$
	N1	H1b	O2	2.18	2.979(4)	152	$1/2 + x, 1/2 + y, z$
	O2	H1w	O1	1.97	2.805(4)	177	x, y, z
	O2	H2w	O2	2.51	2.809(4)	102	$-x, y, 1/2 - z$
6	N1	H1a	N2a	2.24	3.099(6)	168	$-1 - x, -y, -z$
	N1a	H1a	N2	2.29	3.161(6)	174	$-1 - x, -y, -z$
	C8	H8	Br1	3.03	3.628(5)	123	$-x, 1 - y, -z$
	C6	H6	Br2	2.95	3.858(4)	163	$-x, 1 - y, 1 - z$
	C17	H17	Cg(C3a–C8a)^a	2.88	3.576(7)	132	x, y, z
9	N1	H1a	N2	2.25	3.112(5)	173	$1 - x, -y, -z$
	C8	H8	Cl	2.93	3.618(5)	131	$-x, 1 - y, -z$
	C6	H6	Cl	2.95	3.883(4)	169	$1 - x1 - y, -z$

^{a} Cg = centroid of indicated aromatic ring.

IR spectra

Selected IR bands and their assignments are presented in Table 5. The ν(NH$_2$), ν(C=N–N=C) and ν(Sn–C) bands have been identified based on literatures values.[39,40] The ν(NH$_2$)$_{asym}$ and ν(NH$_2$)$_{sym}$ stretching vibrations of the ligands appear in the range 3234–3442 cm^{-1}. These bands do not shift significantly upon complex formation, indicating that the amino nitrogen atom is not involved in coordination
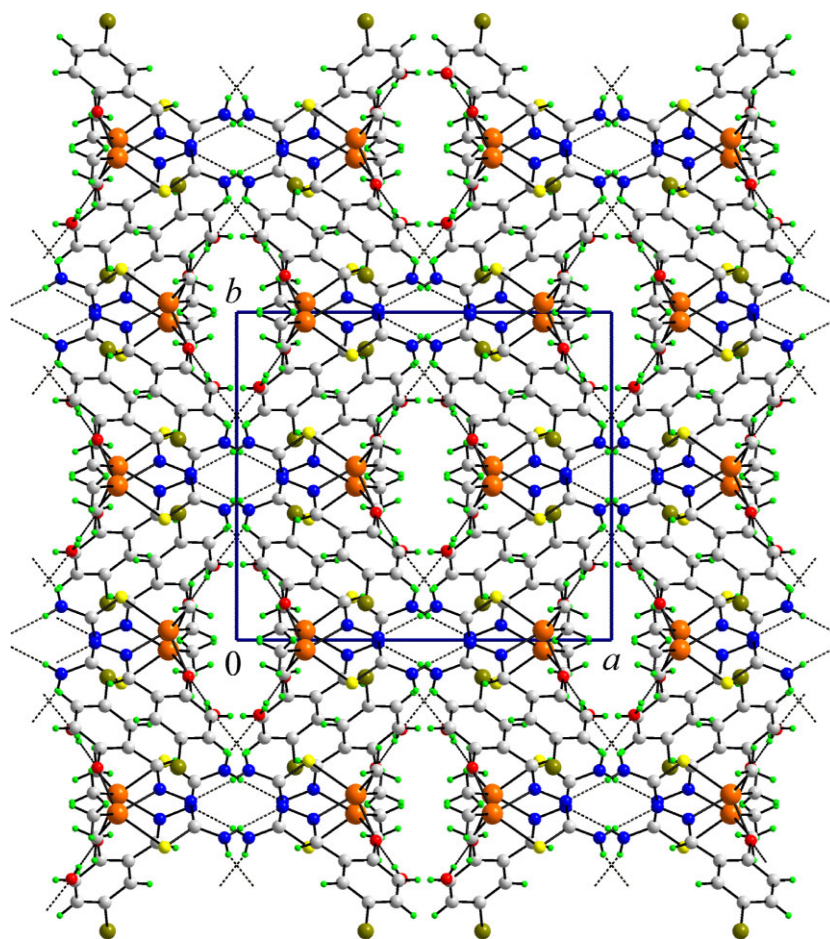
Figure 8. View of the unit cell contents of [Me$_2$SnL^2].OH$_2$ (**4**) along the *c*-axis. This figure is available in colour online at www.interscience.wiley.com/AOC.

with tin. The spectra show medium to strong absorptions within the range 1600–1651 cm^{-1} due to ν (C=N–N=C).[40] The ν(Sn–C)$_{asym}$ and ν(Sn–C)$_{sym}$ bands appear at 520–540 and 460–480 cm^{-1}, respectively. In the spectrum of **4**, a broad band in the range 3290–3410 cm^{-1} is observed which indicates the presence of OH stretching vibrations along with the

NH$_2$ stretching vibrations, consistent with **4** crystallizing as a hydrate.

NMR spectra

The ^{1}H NMR data for **1–9** are presented in Table 6. The observed resonances were assigned on the basis of their

Table 5. IR spectral data (cm^{-1}) for **1–9**[a]

	ν(NH$_2$)$_{asym}$	ν(NH$_2$)$_{sym}$	ν(C=N–N=C)	ν(Sn–C)	ν(Sn–S)
1	3300(w)	3124(w)	1651(s)	536(m), 478(w)	340(m)
2	3307(w)	3151(w)	1645(m)	532(w), 461(s)	342(m)
3	3446(w)	3340(w)	1604(m)	530(w), 475(w)	342(m)
4	3290–3410(b,w)		1633(m)	521(w), 475(w)	347(m)
5	3302(w)	3158(m)	1620(m)	525(w),470(w)	345(m)
6	3452(w)	3292(w)	1622(m)	535(w), 480(w)	342(m)
7	3433(m)	3280(w)	1606(m)	520(w), 475(w)	338(m)
8	3300(s)	3168(s)	1600(s)	538(w),480(w)	350(m)
9	3452(w)	3292(w)	1624(m)	540(w),485(w)	345(m)

[a] s, strong; m, medium; w, weak; b, broad.

integration and multiplicity patterns. The ligand and tin-bound organic group protons give signals in the expected ranges.[30,41,42] The spectra of the diphenyltin compounds **3**, **6** and **9** show complex patterns for the aromatic protons (both ligand and SnPh). In compound **3** the C–H and aromatic protons appear as complex multiplets in the range 8.40–6.50 ppm. The C–H proton of CH═N has been identified at 8.31 ppm. Spin–spin coupling between the tin nucleus and the azomethine-proton, ^3J(SnN═CH), was detected in all spectra, thereby confirming the presence of nitrogen–tin coordination. In addition, the values of the coupling constants for ^3J(SnN═CH), i.e. 33–45 Hz, ^2J(SnCH$_3$), 69–73 Hz, are within the ranges reported for penta-coordinated organotin(IV) complexes with ONO and ONS tridentate Schiff bases.[15] Solution ^{13}C and ^{119}Sn NMR data of the complexes in CDCl$_3$ are presented in Table 7. The number of ^{13}C signals found corresponds with the number of magnetically non-equivalent carbon atoms. Contrary to the literature,[29,30] it is proposed that the C-2 signal (attached to a phenyl group and a ═N–N═ moiety) is the most deshielded carbon atom followed by C-1 (attached to two N atoms and a –S–Sn moiety) and then by the C-8 carbon of the phenyl ring of the ligand. The weak satellites associated with the C-8 carbon atom are assigned to ^2J(^{119}Sn–O–^{13}C)[43] rather than the ^2J(^{119}Sn$\cdots$N–^{13}C), as indicated by Casas and co-workers.[30] The ^{119}Sn shifts and ^1J(^{119}Sn–^{13}C) coupling values are indicative of penta-coordination around the tin atom.[44]

Electronic and fluorescent spectra

Visible and fluorescent spectra of selected compounds are recorded in Tables 8 and 9. As expected, in the visible region the electronic spectra show one broad absorption of medium intensity. The yellow colour is due to the $n - \pi^*$ transition of the thiosemicarbazide chromophore. Interestingly, the compounds are fluorescent under ordinary conditions. At this time it is difficult to conclusively indicate what the origin of this property is. However, detailed studies are in progress.
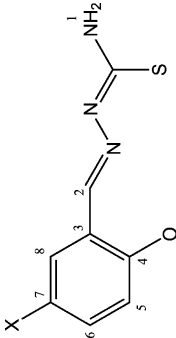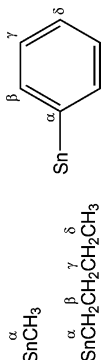
Evaluation of biological properties

Anti-microbial activities

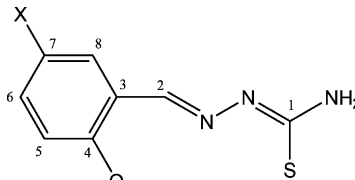The anti-microbial properties of the organotin compounds were evaluated and results are summarised in Tables 10
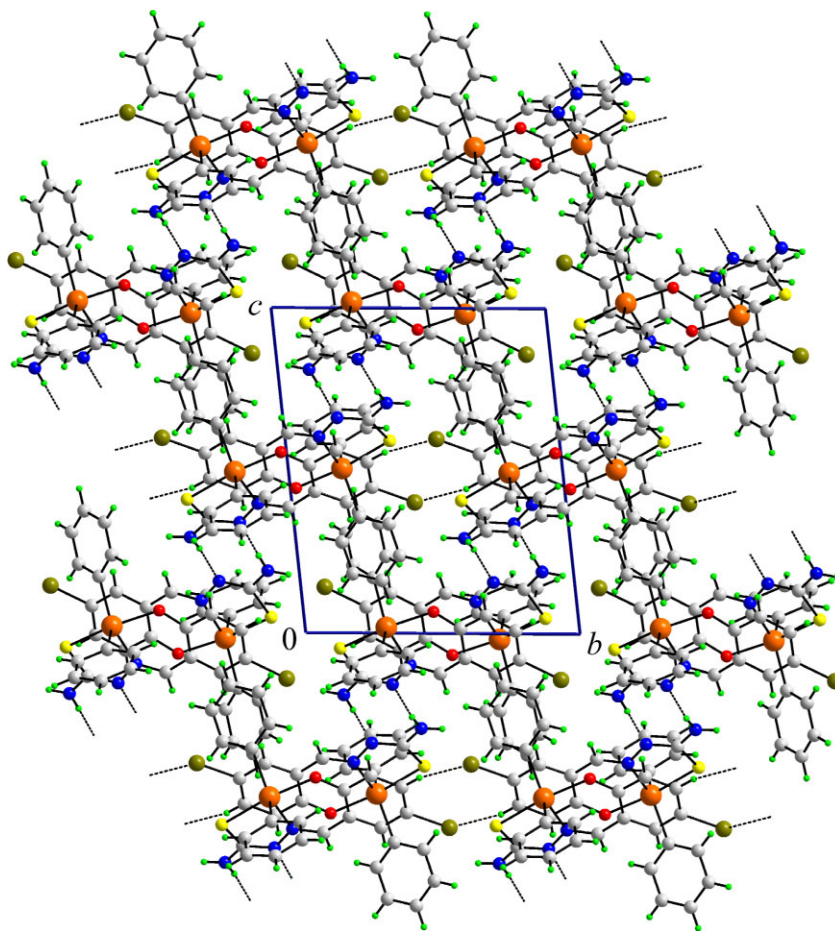
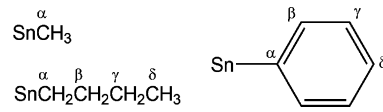**Figure 9.** View of the unit cell content of [Ph$_2$SnL^2] (**6**) down the *a*-axis. This figure is available in colour online at www.interscience.wiley.com/AOC.

Table 6. ¹H NMR chemical shifts and coupling data (ppm and Hz) for **1–9**[a]

	H-1	H-2	H-5	H-6	H-7	H-8	H-α (SnCH₃) / (SnCH₂CH₂CH₂CH₃)	H-β	H-γ	H-δ
1	5.10 (s, 2H)	8.49 (s, 1H)[40][c]	6.78–6.76 (d, 1H)	7.29 (m, 1H)	6.72 (t, 1H)	7.12–7.09 (d, 1H)	0.87 (s, 6H) [72][d]	—	—	—
2	4.97 (s, 2H)	4.48 (s, 1H)[37.5][c]	6.78–6.75 (d, 1H)	7.29 (m, 1H)	6.69 (t, 1H)	7.10–7.08 (d, 1H)	1.82–1.61 (m, 4H)	1.55–1.42 (m, 4H)	1.34 (m, 4H)	0.87 (t, 6H)
3	4.47 (s, 2H)	8.24 (s, 1H)	6.63–6.61 (d, 1H)	7.28 (m, 1H)	6.52 (m, 1H)	7.28 (d, 1H)	—	8.27	7.23	7.23
4	5.02 (s, 2H)	8.40 (s, 1H)[39][c]	6.68–6.65 (d, 1H)	7.35–7.31 (d, 1H)	—	7.21–7.20 (s, 1H)	0.87 (s, 6H) [70/73][d]	—	—	—
5	5.18 (s, 2H)	8.37 (s, 1H)[39][c]	6.67–6.64 (d, 1H)	7.30 (d, 1H)	—	7.18–7.17 (s, 1H)	1.69–1.57 (m, 4H)	1.55–1.49 (m, 4H)	1.42–1.25 (m, 4H)	0.87 (t, 6H)
6	4.33 (s, 2H)	7.96 (s, 1H) [n.d.][b]	6.66–6.65 (d, 1H)	6.83–6.80 (d, 1H)	—	7.31–7.17 (s, 1H)	—	8.33–8.03 (m, 4H)	7.31–7.17 (m, 4H)	7.31–7.17 (m, 2H)
7	5.14 (s, 2H)	8.39 (s, 1H)[38][c]	6.72–6.70 (d, 1H)	7.26–7.19 (d, 1H)	—	7.07–7.06 (s, 1H)	0.87 (s, 6H) [71/74][d]	—	—	—
8	5.00 (s, 2H)	8.39 (s, 1H)[34][c]	6.72–6.69 (d, 1H)	7.22–7.18 (d, 1H)	—	7.05–7.04 (s, 1H)	1.69–1.59 (m, 4H)	1.55–1.44 (m, 4H)	1.42–1.26 (m, 4H)	0.87 (t, 6H)
9	5.10 (s, 2H)	8.41 (s, 1H)[44][c]	7.05–6.97 (d, 1H)	7.05–6.97 (d, 1H)	—	7.44–7.24 (s, 1H)	—	8.01–7.65 (m, 4H)	7.44–7.24 (m, 4H)	7.44–7.24 (m, 2H)

[a] Spectra recorded in CDCl₃ except for compounds **3** and **6** which were measured in C₆D₆. Multiplicity is given as s, singlet; d, doublet; t, triplet; m, multiplet.
[b] n.d. = not detected.
[c] ^3J (Sn–H) Hz.
[d] ^2J ($^{117/119}$Sn–CH₃) Hz.

Table 7. ^{13}C and ^{119}Sn NMR chemical shifts and coupling data (ppm and Hz) for **1–9**[a]

	[119]Sn	C-1	C-2	C-3	C-4	C-5	C-6	C-7	C-8	C-α	C-β	C-γ	C-δ
1	−102.5	165.85	167.94	121.39	160.62 [20.17]g	116.77	133.55	117.16	134.6	5.94 [595.90]b	—	—	—
2	−120.2	166.62	168.18	121.41	160.86 [16.80]g	116.69	133.61	116.77	133.66	25.86 [562.50]b	27.41 [30.80]c	26.46 [90.0]d	13.58
3	−232.4	166.21	166.72	121.70	161.03 [20.4]g	116.83	133.83	117.43	134.97	142.49 [865.3]b	135.78 [56.32]c	128.65 [82.35]d	129.98 [16.72]e
4	−98.0	164.98	168.45	123.47	159.21 [20.12]g	108.19	134.88	118.39	137.07	5.98 [593.10]b	—	—	—
5	−116.4	165.28	168.79	123.19	158.83 [16.82]g	107.69	134.74	118.37	136.82	25.84 [557.60]b	27.30 [30.75]c	26.35 [64.50]d	13.53
6	−229.4	165.48	166.81	123.61	159.26 [18.6]g	108.41	135.04	118.36	136.09	142.08 [843.75]b	135.71 [57]c	128.74 [82.5]d	130.1 [16.87]e
7	−98.1	164.33	168.50	122.93	159.01 [20.25]g	117.55	131.73	121.39	134.25	5.98 [592.90]b	—	—	—
8	n.m.f	164.91	168.79	122.39	158.93 [16.88]g	117.60	131.67	120.93	134.15	25.82 [558.1]b	27.31 [30.63]c	26.37 [81.0]d	13.5
9	−229.3	165.13	166.83	123.23	159.52 [20.25]g	117.62	131.99	121.08	134.59	142.14 [807.69]b	135.73 [56.4]c	128.75 [82.65]d	130.14 [16.57]e

[a] Spectra recorded in CDCl$_3$ solution.
[b] $^1J(^{13}C-^{119}Sn)$ in Hz.
[c] $^2J(^{13}C-^{119}Sn)$ in Hz.
[d] $^3J(^{13}C-^{119}Sn)$ in Hz.
[e] $^4J(^{13}C-^{119}Sn)$ in Hz.
[f] n.m. = not measured.
[g] $^2J(^{119}Sn-O-^{13}C)$ in Hz

and 11. It was observed that all the test compounds inhibit bacterial growth to varying extent. Compound **1** was found to be least potent among the four compounds tested. With the exception of *S.aureus* it had no effect on the different Gram-negative bacteria chosen for the study. However, it inhibited the growth of Gram-positive bacteria *B. subtilis* and *L. rhamnosus* when tested at high concentrations.

Table 8. Electronic absorption spectra of selected compounds recorded in methanol solution

	λ_{max} (nm)
1	392
3	390
4	405
6	403
7	397
9	398

Table 9. Fluorescence data of selected compounds recorded in methanol solution

	Excitation (nm)	Emission (nm)
1	451.4	489.5
2	357.0, 451.4	491.3
3	308.0, 357.0, 445.9	487.7
4	373.3, 455.0	494.7
6	318.2, 366.1, 455.0	498.6
7	373.2, 459.6	490.3
9	311.6, 366.1, 453.2	493.1

When the anti-fungal properties of the compounds were evaluated it was observed that compound **4** was effective against all the four fungi selected in the study with the minimum MIC values obtained for *A. porri* and *M. phaseolina* (MIC 1.78 µg ml^{-1}). Compound **6** was effective against all the pathogenic fungi except *D. oryzae*, while **1** was effective against *A. porri* and *M. phaseolina* (MIC 3.76 µg ml^{-1}) and **3** was
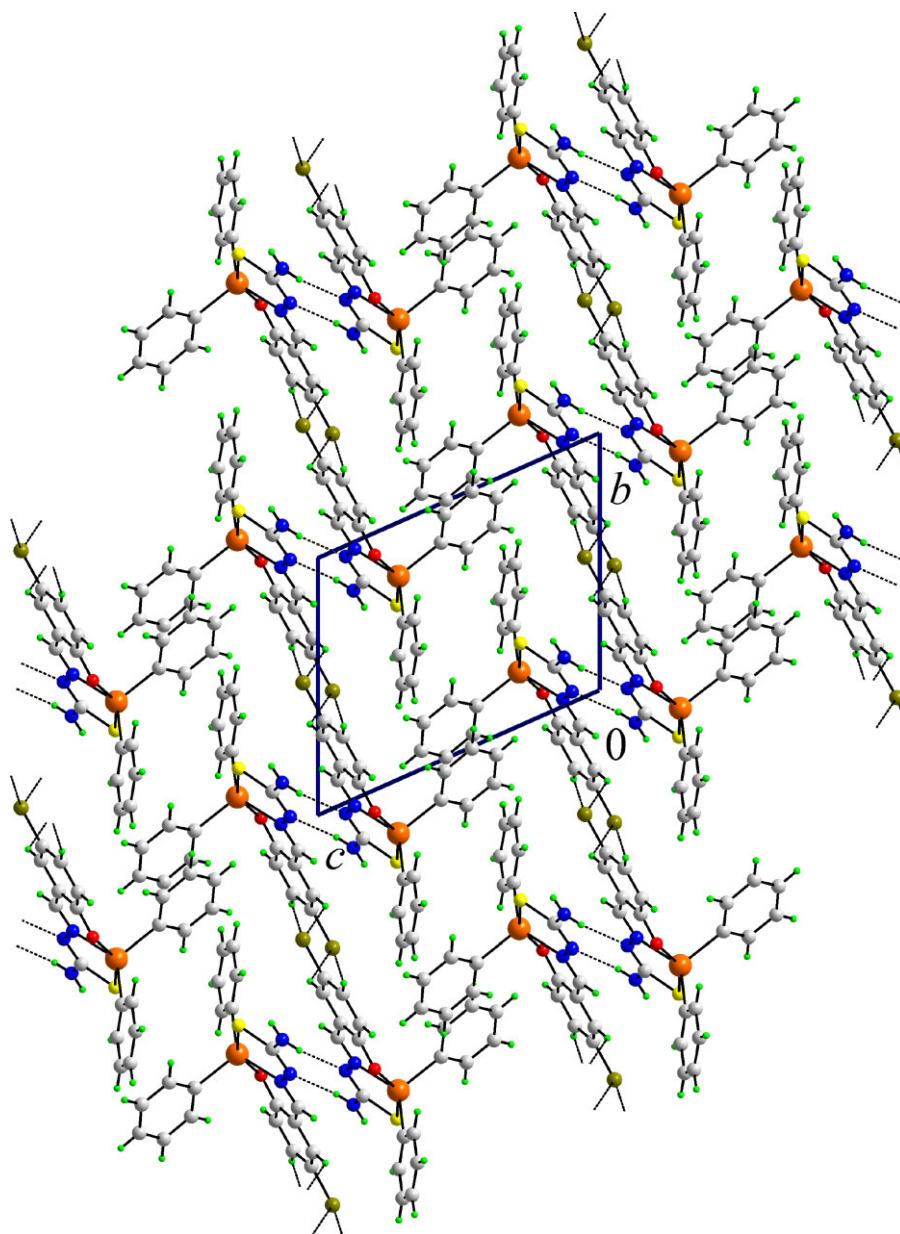
Figure 10.   View of the unit cell content of [Ph$_2$SnL^3] (**9**) down the *a*-axis. This figure is available in colour online at www.interscience.wiley.com/AOC.

Table 10.   Fungicidal activity of selected compounds against different fungi species — effects on spore germination[a]

	Minimum inhibitory concentration (µg ml^{-1})			
	C. eragrostidis	*A. porri*	*D. oryzae*	*M. phaseolina*
1	37.6	3.76	376	3.76
3	440	4.4	440	44
4	17.8	1.78	17.8	1.78
6	18.4	1.84	184	18.4

[a] The reported values represent the mean determined from three experiments. MIC values above 30 µg ml^{-1} were not considered significant.

effective only against *A. porri* (MIC 4.4 µg ml^{-1}). The study indicates that the alkyltin derivatives are more active than the aryltin compounds for both bacteria and fungi in accord with the literature conclusions.[45] It is not possible from this study to determine the structure–activity relationship (SAR) between the anti-microbial activity and structure of organotins used or suggest any specific mode of action of the organotins on the bacteria or fungi selected. However, earlier studies have suggested that charged metabolites of the organotins could play a role in their anti-microbial activities.[46] Moreover, the chelating potential of organotins could also be responsible for the enhanced anti-microbial activity observed.[47,48] The

variation in the anti-microbial properties against different organisms observed probably depends on the impermeability of the cell or differences in ribosomes to the organotins used.[49] Further studies with bacteria and fungi are in progress to determine the mode of action of these compounds.

Phytotoxic properties

The phytotoxic effects of selected organotin compounds were studied on three economically important crops, namely *Oryzae sativa* (IR-8), *Lens culinaris* and *Cicer aurantinum* (Table 12). None of the organotin compounds demonstrated useful phytotoxicity as they did not affect seed germination.

Cytotoxicity

The cytotoxic effects of several organotin compounds were examined against several human cancer cell lines *in vitro* by SRB assay. Amongst the different organotin compounds selected for the study, compound **3** was found to possess the highest potency against most of the cell lines studied followed by compound **6** (Table 13). Compound **4** appeared

Table 11. Effect of different organotin compounds on bacterial growth[a]

	a	b	c	d	e	f	g	h
1	n.e.	n.e.	n.e.	n.e.	n.e.	32.58	22.28	45.00
3	5.50	20.12	26.38	40.53	30.28	6.50	n.e.	2.02
4	28.88	35.55	17.07	13.35	37.20	40.00	n.e.	6.05
6	12.50	26.40	32.40	32.96	17.52	40.70	n.e.	23.10

[a] The doses mentioned represent the minimum effective dose needed to inhibit 50% growth of bacteria. MIC values above 50 µg ml^{-1} were not considered significant. n.e. = no effect. The values represent the mean of three experiments.
[b] **a**, *A. hydrophila*; **b**, *S. typhi*; **c**, *S. typhimurium*; **d**, *S. flexnri*; **e**, *E. coli*; **f**, *B. subtilis*; **g**, *S. aureus*; **h**. *L. rhamnosus*.
ED_{50} = effective dose (µg ml^{-1}).

Table 12. Phytotxic effect (µg/ml) of selected organotin compounds[a,b]

| | | Percentage germination after treatment for | | | | | | | | |
| | | 1 h | | | 4 h | | | 12 h | | |
	Concentration	a	b	c	a	b	c	a	b	c
1	100	92	82	96	92	82	94	93	80	93
	50	95	83	95	94	85	94	94	80	92
	25	92	81	95	92	80	95	95	81	91
3	100	94	86	96	94	87	95	95	85	96
	50	94	88	94	95	87	96	95	85	98
	25	96	83	96	96	81	95	96	84	97
4	100	96	80	94	96	81	95	96	80	95
	50	94	82	93	94	81	93	94	83	93
	25	95	80	92	94	80	92	94	79	92
6	100	94	90	97	93	91	95	91	90	95
	50	93	92	96	94	90	94	93	91	94
	25	92	90	97	92	90	95	90	91	96
Control[c]		96	81	98	94	80	97	95	80	96

[a] The phytotoxicity of the compounds was checked by seed germination assays. Seeds were incubated with different concentrations of the compounds for 1, 4 and 12 h, washed to remove the excess unbound compounds and the percentage germination checked following incubation for 72 h. Control seeds exhibited 95–100% germination efficacy. Values represent mean of three experiments.
[b] **a**, *Cicer aurantinum*; **b**, *Lens culinaris*; **c**, *Oryzae sativa*.
[c] The control seeds were incubated in DMSO/water for the indicated time period.

to be the least potent, only inducing significant cell death against Colo205 (88.3%). It is interesting to note that, in contrast to earlier reports on hexa-coordinated compounds,[50] this study reports phenyl derivatives to be more active than the butyl derivatives. The reason behind the wide spectrum of cytotoxicity observed for the organotins in

Table 13. Cytotoxicity scores (µg ml^{-1}) of selected organotin compounds against cell lines by SRB assay. Compounds inducing less than 50% cell death were not considered significant

| | | Percentage growth inhibition | | | | | | | | | | | |
| | | **1** | | | **3** | | | **4** | | | **6** | | |
Cell line	Origin	10	20	40	10	20	40	10	20	40	10	20	40
Colo205	Colon	32.9	84.8	95.6	93.9	94.8	92.7	88.3	91.0	87.1	69.5	93.2	94.7
Hop62	Lung	43.1	63.1	76.5	83.0	88.2	90.3	45.9	60.1	70.9	41.7	80.2	62.6
MCF7	Breast	74.0	75.1	75.1	82.2	84.4	83.0	53.8	57.8	70.4	76.1	82.9	84.8
PC3	Prostate	37.6	72.4	83.3	86.4	87.7	92.6	13.8	23.0	47.3	85.0	88.5	83.9
SiHa	Cervix	28.6	66.0	70.3	79.4	81.2	85.3	0.0	45.9	59.1	84.9	87.9	90.2
ZR-75-1	Breast	27.6	57.6	85.9	16.0	95.9	96.1	1.8	40.5	47.2	46.8	88.7	91.7
A-2780	Ovarian	86.6	88.8	86.1	90.0	91.8	88.0	73.0	84.6	87.5	94.7	86.0	87.9
DWD	Throat	82.3	79.4	76.1	83.8	87.4	90.8	0.0	49.6	52.9	0.6	26.2	51.7
K562	Leukaemia	35.2	28.1	40.6	60.3	61.2	62.0	13.2	11.2	21.4	4.1	39.1	34.4
DU145	Prostate	24.4	65.6	77.6	79.2	87.9	89.1	52.3	74.5	85.1	41.8	80.0	85.5

this study is not known at present. The results further suggest that the compounds are not equally effective against all the cell lines selected. This difference in the degree of selectivity could, presumably, be either due to differential binding potential of the compounds or metabolic activities of the cell lines, which helps in overcoming the cytotoxic effects of the organotins. Organotins offer the potential of reduced cytotoxicity, non-cross resistance and a different spectrum of activity compared with conventional chemotherapeutic agents such as platinum-containing compounds.[27,46,51] The organotins selected for this study appear to be attractive anti-cancer candidates because of the low doses required that minimize the chances of toxic side effects. From the available literature and our own observations it appears that the organotins described herein exert their cytotoxic effect at much lower doses compared with cisplatin[52–54] in the evaluated cell lines and adriamycin, which was used as positive control in this study. We now plan to extend the experiments at further lower concentrations under comparable conditions with standard controls.

The exact mechanism of action of organotins on controlling tumour growth is not well known.[28] It has been reported that organotins induce tumour cell death in a dose-dependent manner.[55–57] At higher concentrations, these compounds induce degenerative changes indicative of necrosis accompanied by random DNA breakdown. Electron microscopic studies revealed organotin-induced cytotoxicity to be associated with cell shrinkage, chromatin condensation, fragmentation of DNA and development of apoptotic bodies.[49] It has been suggested that organotins, like other DNA binding drugs, induce cellular stress which activates the tumour suppressor p53 leading to apoptotic death.[49] The involvement of zinc- and calcium-dependent endonucleases has also been suggested in cytotoxicity induced by organotins.[58] Our on-going effort aims to determine the mode of action of these compounds on the sensitive cancer cell lines.

Acknowledgements

REFERENCES

1. Nath M, Yadav R, Eng G, Nguyen TT, Kumar A. *J. Organomet. Chem.* 1999; **577**: 1.
2. Kamruddin Sk, Chattopadhyaya TK, Roy A, Tiekink ERT. *Appl. Organomet. Chem.* 1996; **10**: 513.
3. Ahmad F, Parvez M, Ali S, Mazhar M, Munir A. *Synth. React. Inorg. Met.-Org. Chem.* 2002; **32**: 665.
4. Smith FE, Hynes RC, Ang TT, Khoo LE, Eng G. *Can. J. Chem.* 1992; **70**: 1114.
5. Goh NK, Khoo LE, Mak TCW. *Polyhedron* 1993; **12**: 925.
6. Yin HD, Chen SW. *Inorg. Chim. Acta* 2006; **359**: 3330.
7. Barbieri RS, Beraldo HO, Filgueiras CAL, Abras A, Nixon JF, Hitchcock PB. *Inorg. Chim. Acta* 1993; **206**: 169.
8. Lee FL, Gabe EJ, Khoo LE, Eng G, Smith FE. *Polyhedron* 1990; **9**: 653.
9. Tiwari R, Srivastava G, Crowe AJ, Mehrotra RC. *Inorg. Chim. Acta* 1986; **111**: 167.
10. Saxena A, Tandan JP, Molloy KC, Zuckerman JJ. *Inorg. Chim. Acta* 1982; **63**: 71.
11. Lee FL, Gabe EJ, Khoo LE, Leong WH, Eng G, Smith FE. *Inorg. Chim. Acta* 1989; **166**: 257.
12. Preut H, Huber F, Haupt HJ, Cefalu R, Barbieri R. *Z. Anorg. Allg. Chem.* 1974; **410**: 88.
13. Preut H, Huber F, Barbieri R, Bertazzi N. *Z. Anorg. Allg. Chem.* 1976; **423**: 75.
14. Ghose BN. *Synth. React. Inorg. Met.-Org. Chem.* 1982; **12**: 835.
15. Iskander MF, Labib L, Nour El-Din MMZ, Tawfik M. *Polyhedron.* 1989; **8**: 2755.
16. Mehrotra RC, Srivastava G, Saraswat BS. *Rev. Silicon, Germanium, Tin and Lead Compounds* 1982; **6**: 171.
17. Sengupta P, Dinda R, Ghosh S. *Trans. Met. Chem.* 2002; **27**: 665.
18. Koley AP, Purohit S, Prasad LS, Ghosh S, Manoharan PT. *Inorg. Chem.* 1992; **31**: 305.
19. Laughlin LJ, Young CG. *Inorg. Chem.* 1996; **35**: 1050.
20. Holm RH. *Coord. Chem. Rev.* 1990; **100**: 183.
21. Basuli F, Ruf M, Pierpont CG, Bhattacharya S. *Inorg. Chem.* 1998; **37**: 6113.
22. Basuli F, Peng SM, Bhattacharya S. *Inorg. Chem.* 1997; **36**: 5645.
23. Padhye SB, Kauffman GB. *Coord. Chem. Rev.* 1985; **63**: 127.
24. Haiduc I, Silvestru C. *Coord. Chem. Rev.* 1990; **99**: 253.
25. Kamruddin Sk *Ph.D. Thesis.* North Bengal University, West Bengal, India, 1996.
26. Ayoko AG, Bonire JJ, Abdulkadir SS, Olurinola PF, Ehinmidu JO, Kokot S, Yiasel S. *Appl. Organomet. Chem.* 2003; **17**: 749.
27. Moebus VJ, Stein R, Kieback DG, Runnebaum IB, Sass G, Kreienberg R. *Anticancer Res.* 1997; **17**: 815.
28. Gielen M, Tiekink ERT. *Metallotherapeutic Drugs and Metal-based Diagnostic Agents: the Use of Metals in Medicine*, Chapter 22, Gielen M, Tiekink ERT (eds). Wiley: Chichester, 2005; 421.
29. Saxena A, Tandon JP. *Polyhedron* 1984; **3**: 681.
30. Casas JS, Sanchez A, Sordo J, Vazquez-Lopez A, Castellano EE, Zukerman-Schpector J, Rodriguez-Arguelles MC, Russo U. *Inorg. Chim. Acta* 1994; **216**: 169.
31. Ng SW, Kumar Das VG, Luo BS, Mak TCW. *Z. Kristallogr.* 1994; **209**: 961.
32. Majumdar T, Ghosh S, Pal J, Mazumder S. *Aquaculture* 2006; **256**: 95.
33. Rouxel T, Sarniguet A, Kollmann A, Bousquet JF. *Physiol. Mol. Plant Pathol.* 1989; **34**: 507.
34. Skehan P, Storeng R, Scudiero A, Monks J, McMohan J, Vistica D, Warren JT, Bokesch H, Kenney S, Boyd MR. *J. Natl Cancer. Inst.* 1990; **82**: 1107.
35. Beurskens PT, Admiraal G, Beurskens G, Bosman WP, García-Granda S, Smits JMM, Smykalla C. The DIRDIF Program System, Technical Report of the Crystallography Laboratory, University of Nijmegen, 1992.
36. Sheldrick GM. *SHELXL-97, Program for the Crystal Structure Refinement*. University of Göttingen: Göttingen, 1997.
37. Johnson CK. ORTEP. Report ORNL-5138; Oak Ridge National Laboratory, TN, 1976.
38. DIAMOND, Visual Crystal Structure Information System, Version 3.1d, Crystal Impact, Bonn, 2006.
39. Silverstein RM, Bassler GC, Morrill TC. *Spectrometric Identification Of Organic Compounds*, 5th edn. Wiley: Toronto, 1991.
40. Labib L, Khalil TE, Iskander MF, Refaat LS. *Polyhedron* 1996; **15**: 3697.
41. Basu Baul TS, Dutta S, Rivarola E, Scopelliti M, Choudhuri S. *Appl. Organomet. Chem.* 2001; **15**: 947.

42. Martinez EG, Sanchez Gonzalez A, Casas JS, Sordo J. *J. Organomet. Chem.* 1993; **453**: 47.
43. Pham HV, Rusterholz B, Pretsch E, Simon W. *J. Organomet. Chem.* 1991; **403**: 311.
44. Ahmad F, Ali S, Parvez M, Munir A, Mazhar M, Khan KM, Shah TA. *Heteroatom Chem.* 2002; **13**: 638.
45. Poller RC. *The Chemistry of Organotin Compounds*, Logos Press: London, 1970; 274.
46. Winship KA. *Adverse Drug React. Acute Poisoning Rev.* 1988; **7**: 19.
47. Cooney JJ, Wuertz S. *J. Ind. Microbiol. Biotechnol.* 1989; **4**: 375.
48. Rehman S, Ali S, Mazhar M, Badshah A, Parvez M. *Heteroatom Chem.* 2006; **17**: 420.
49. Singh HL, Varshney AK. *Bioinorg. Chem. Appl.* 2006; DOI 10.1155/BCA/2006/23 245.

50. Li Q, da Silva MFCG, Pombeiro AJL. *Chem. Eur. J.* 2004; **10**: 145.
51. Barbieri F, Viale M, Sparatore F, Schettini G, Favre A, Bruzzo C, Novelli F, Alama A. *Anti-Cancer Drugs* 2002; **13**: 599.
52. Zamble DB, Jacks T, Lippard SJ. *Proc. Natl Acad. Sci.* 1998; **95**: 6163.
53. Lan FQ, Irne OLN. *Cancer Lett*, 2002; **175**: 27.
54. Hoti N, Ma J, Tabassum S, Wang Y, Wu M. *J. Biochem.* 2003; **134**: 521.
55. Zaucke F, Zoltzer H, Krug HF. *Fresenius J. Anal. Chem.* 1998; **361**: 386.
56. Barbieri F, Viale M, Sparatore F, Favre A, Cagnoli M, Bruzzo C, Novelli F, Alama A. *Anticancer Res.* 2000; **20**: 977.
57. Chou RH, Huang H. *Biochem. Biophys. Res. Commun.* 2002; **26**: 298.
58. Cima F, Ballarin L. *Appl. Organomet. Chem.* 1999; **13**: 697.